Study of energy transfer in silicon-based micro-ring resonators*

LI Xin-juan (李昕娟)**, **WU Rong** (吴蓉), **HU Yu-feng** (胡玉峰), **HU Li-xin** (胡立新), **and GUO Jian-cheng** (郭建成)

School of Electronic and Information Engineering, Lanzhou Jiaotong University, Lanzhou 730070, China

(Received 20 June 2014)

Physical model, time-domain model, transmission spectra and energy transfer diagram of silicon-based micro-ring resonators based on the parallel waveguide structure are analyzed in this paper, in which transmission spectrum is obtained by Matlab, and the energy transfer process is analyzed by Rsoft. According to the analyses of the models and results, the energy transfer process in this type of resonator is clear to a great extent. The experimental results show that when the input signal is stable, the energy of the micro-ring resonator and the drop port tends to be steady after the input optical signal is coupled in the coupling region, which proves that the silicon-based micro-ring resonators can select specific optical signal if the input optical signal satisfies the resonance condition. However, if the resonance condition is not met, filtering function, optical switch function and signal selection function can be realized. Therefore, the analysis and simulation of energy transfer in silicon-based micro-ring resonators can not only enrich the silicon micro-ring resonator theory, but also provide new theoretical basis and method for the design and optimization of existing optoelectronic devices.

Document code: A **Article ID:** 1673-1905(2014)05-0321-4

DOI 10.1007/s11801-014-4111-x

Silicon-based photonics is an important direction in the development of optoelectronic devices[1,2]. After Marcatili[3] proposed the concept and structure of micro-ring resonator, a lot of researches[4-6] about micro-ring have been made by many institutes and research centers. Numerous achievements of the researches are presented in terms of optical switches, optical encoders and optical routers[7-12]. The internal energy transmission characteristics of silicon-based micro-ring resonator are often rendered by Matlab, which cannot characterize the process distinctly.

In this paper, the process of energy transmission in silicon-based micro-ring resonator based on the parallel waveguide structure is studied by analyzing the physical model, the time-domain model, transmission spectra and energy transfer diagram. According to the internal energy transfer process of the devices performed by Rsoft, the internal mechanism can be grasped. At the same time, the new theory and method can be provided for the design of new optoelectronic devices and the performance optimization of photoelectronic devices in the future.

The directional coupler and the transmission line are two basic elements of the silicon-based micro-ring resonator[13], and the physical models of these two devices are shown in Fig.1[14].

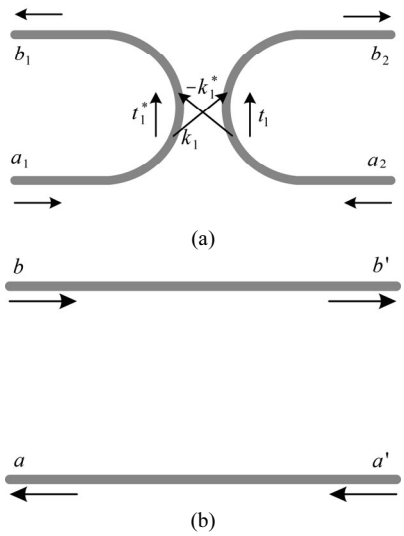

Fig.1 Physical models of (a) directional coupler and (b) transmission line

According to Fig.1(a), the transmission in the directional coupler can be expressed as

$$\begin{bmatrix} b_1 \\ b_2 \end{bmatrix} = \begin{bmatrix} t_1^* & -k_1^* \\ k_1 & t_1 \end{bmatrix} \begin{bmatrix} a_1 \\ a_2 \end{bmatrix}. \tag{1}$$

* This paper has been supported by the National Natural Science Foundation of China (No.61366006).

** E-mail: lilyness@163.com

By derivation, the transfer matrix of directional coupler is

$$\boldsymbol{J}=\begin{bmatrix}1/k_1 & -t_1/k_1\\ t_1^*/k_1 & -1/k_1\end{bmatrix}. \tag{2}$$

According to Fig.1(b), the transmission in the transmission line is

$$\begin{bmatrix}b'\\ a'\end{bmatrix}=\begin{bmatrix}\alpha^{1/2}\exp(\mathrm{j}\theta/2) & 0\\ 0 & \alpha^{-1/2}\exp(-\mathrm{j}\theta/2)\end{bmatrix}\begin{bmatrix}b\\ a\end{bmatrix}, \tag{3}$$

where a and b are the input amplitudes, a' and b' are the output amplitudes, α is the single-pass amplitude of transmission factors, and θ is the single-pass phase shift. The transfer matrix of the transmission line is

$$\boldsymbol{K}=\begin{bmatrix}\alpha^{1/2}\exp(\mathrm{j}\theta/2) & 0\\ 0 & \alpha^{-1/2}\exp(-\mathrm{j}\theta/2)\end{bmatrix}. \tag{4}$$

The physical model of the silicon-based micro-ring resonator based on the parallel waveguide structure is shown in Fig.2[14], which has four ports of input port, through port, add port and drop port.

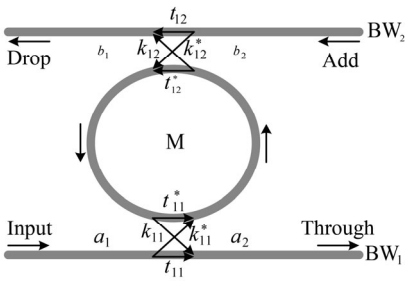

Fig.2 Physical model of the silicon-based micro-ring resonator

The transfer functions of the physical model derived from Eqs.(1)–(4) are

$$A=\frac{b_1}{a_1}=\frac{\alpha_1^{1/2}\cdot k_{11}^*\cdot k_{12}\cdot\exp(\mathrm{j}\cdot\theta_1/2)}{1-\alpha_1\cdot t_{11}^*\cdot t_{12}^*\cdot\exp(\mathrm{j}\cdot\theta_1)}, \tag{5}$$

$$B=\frac{b_2}{a_2}=\frac{\alpha_1^{1/2}\cdot k_{11}\cdot k_{12}\exp(\mathrm{j}\cdot\theta_1/2)}{1-\alpha_1\cdot t_{11}^*\cdot t_{12}^*\exp(\mathrm{j}\cdot\theta_1)}, \tag{6}$$

$$C=\frac{a_2}{a_1}=\frac{t_{11}-\alpha_1\cdot t_{12}^*\exp(\mathrm{j}\cdot\theta_1)}{1-\alpha_1\cdot t_{11}^*\cdot t_{12}^*\cdot\exp(\mathrm{j}\cdot\theta_1)}, \tag{7}$$

$$D=\frac{b_1}{b_2}=\frac{t_{12}-\alpha_1\cdot t_{11}^*\cdot\exp(\mathrm{j}\cdot\theta_1)}{1-\alpha_1\cdot t_{11}^*\cdot t_{12}^*\cdot\exp(\mathrm{j}\cdot\theta_1)}, \tag{8}$$

where k_{11}, k_{11}^*, k_{12} and k_{12}^* are the cross-coupling coefficients, t_{11}, t_{11}^*, t_{12} and t_{12}^* are the self-coupling coefficients, and α_1 is the single-pass amplitude transmission factor. In other words, the amplitudes of a_2 and b_1 can be expressed as

$$b_1=A\cdot a_1+D\cdot b_2, \tag{9}$$

$$a_2=B\cdot b_2+C\cdot a_1. \tag{10}$$

The transfer matrix of micro-ring resonator can be expressed as

$$\boldsymbol{Y}=\begin{bmatrix}1/D & -A/D\\ B/D & (CD-AB)/D\end{bmatrix}. \tag{11}$$

The time-domain model of silicon-based micro-ring resonator is shown in Fig.3. In this model, the electrical fields are time-related functions, and the energy exchange procedure of coupling region can be described by the scattering matrix. Assuming that micro-ring resonator is in a stable state when $t\leq 0$, the amplitudes of $E_2(0)$ and $E_6(0)$ in the two resonant regions with $E_1(0)=1$ can be expressed as

$$E_2(0)=\frac{t_1-\alpha\cdot t_2\cdot\exp(\mathrm{j}\cdot\theta)}{1-\alpha\cdot t_1\cdot t_2\cdot\exp(\mathrm{j}\cdot\theta)}, \tag{12}$$

$$E_6(0)=\frac{-k_1\cdot k_2\cdot\alpha^{1/2}\cdot t_2\cdot\exp(\mathrm{j}\cdot\theta/2)}{1-\alpha\cdot t_1\cdot t_2\cdot\exp(\mathrm{j}\cdot\theta)}. \tag{13}$$

The cross-coupling and the self-coupling coefficients of the field amplitude in the waveguides BW$_1$ and BW$_2$ are assumed to be identical and represented by k_1, k_2 and t_1, t_2, respectively.

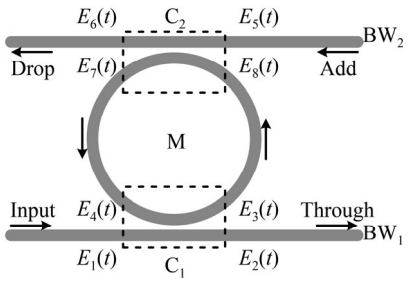

Fig.3 Time-domain model of the silicon-based micro-ring resonator

Schematic diagrams of energy transfer in the silicon-based micro-ring resonator based on the parallel waveguide structure are shown in Fig.4. When the optical signal transfers from the input port to the coupling region C$_1$, the energy which meets resonance condition is coupled into the micro-ring M, and the remaining energy is spread to the through port along the waveguide BW$_1$. The resonance condition of the device can be expressed as

$$m\cdot\lambda_0=n_{\mathrm{eff}}\cdot 2\pi\cdot R, \tag{14}$$

where m represents the series of resonances, λ_0 is the wavelength in vacuum, n_{eff} is the effective refractive index, and R is the radius of the ring waveguide. A filtering device can be designed based on this energy transfer mechanism. The energy transfer process of the device is shown in Fig.4(a) and (b). When the input signal which satisfies the resonance condition reaches the coupling region C$_1$, all energy will be coupled into the micro-ring

M. Depending on the scattering matrix theory and time-domain model, the amplitude of E_2 can be expressed as

$$E_2 = \frac{t_1 - t_2^* \cdot \alpha}{1 - t_1^* \cdot t_2^* \cdot \alpha}. \tag{15}$$

At the same time, there is no signal at the through port. Based on this mechanism, the optical device with switching function can be designed. When the signals reach the coupling region C_2, the optical signals which meet the corresponding resonance condition will be coupled from the ring waveguide M to the straight waveguide BW_1, and then will be output at the drop port. This energy transfer process is shown in Fig.4(c) and (d). Assuming that the optical signals are completely coupled into the straight waveguide BW_2, the amplitude of E_6 can be expressed as

$$E_6 = \frac{-k_1^* \cdot k_2 \cdot \alpha^{1/2}}{1 - t_1^* \cdot t_2^* \cdot \alpha}. \tag{16}$$

Assuming that the micro-ring resonator is symmetrically coupled (k_1=k_2 and t_1=t_2) and there is no loss (α=1), all input optical signals are coupled into the micro-ring M. Then the signals can be coupled into the straight waveguide BW_2 and output at the drop port. The transmission spectra of the device at through port and drop port are shown in Fig.5. Signals obtained from the drop port are the ones that satisfy the resonance condition. Based on this mechanism, the optical device with signal-selection function can be designed.

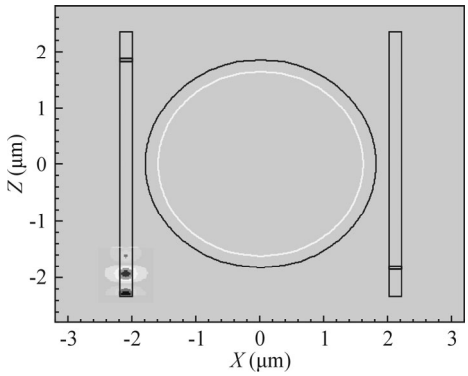

(a) The uncoupling case

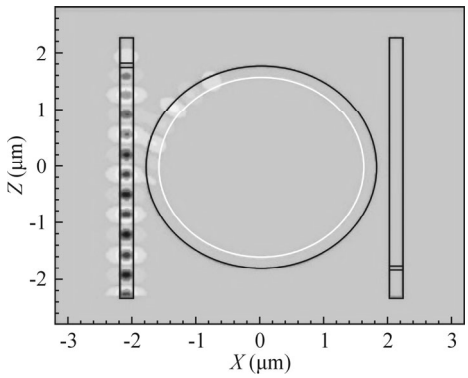

(b) The first energy-coupling case

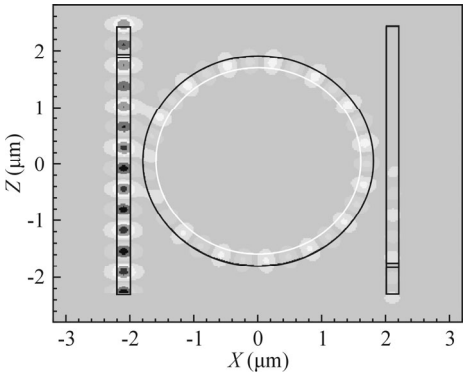

(c) The second energy-coupling case

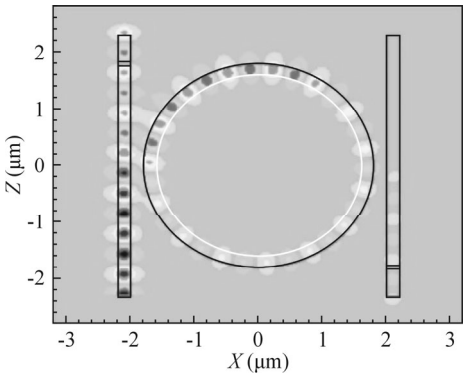

(d) The third energy-coupling case

Fig.4 Schematic diagrams of energy transfer in silicon-based micro-ring resonator based on the parallel waveguide structure

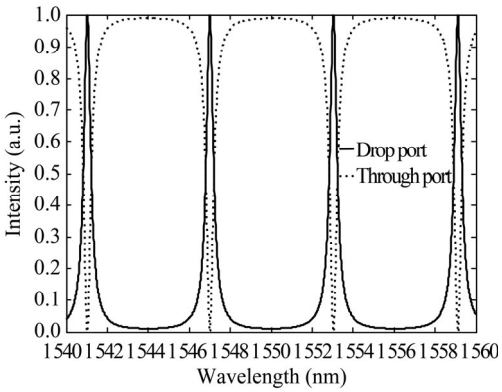

Fig.5 Transmission spectra of the micro-ring resonator based on parallel waveguide structure at through port and drop port

In the case of loss, the output energy at the drop port can be expressed as

$$P_2 = |E_2|^2 \xrightarrow{k_1=k_2, t_1=t_2} P_2 = \left| \frac{t_1 - t_2^* \cdot \alpha}{1 - t_1^* \cdot t_2^* \cdot \alpha} \right|^2. \tag{17}$$

Assuming P_2=0, the critical coupling condition of optical signal in the waveguide can be expressed as

$$\alpha = \left| \frac{t_1}{t_2} \right|. \tag{18}$$

Fig.6 shows the energy transfer diagrams corresponding to Fig.4. In Fig.6(a), because the input optical signals have not entered the coupling region C_1 yet, the output energy of drop port is 0, and there is no energy in micro-ring. In Fig.6(b), optical signals are coupled into the coupling region C_1 but not transferred to the micro-ring coupling region C_2, so there is energy in micro-ring but no energy at drop port. In Fig.6(c), the energy coupled into the micro-ring M reaches the maximum. With the optical signals traveling to the coupling region C_2, the optical signals which meet the resonance condition are coupled into the straight waveguide BW_2, and the output energy at the drop port increases. In Fig.6(d), the energy in the ring waveguide achieves balance with the process of coupling-in and coupling-out, and the energy drops gradually and tends to be steady in the process.

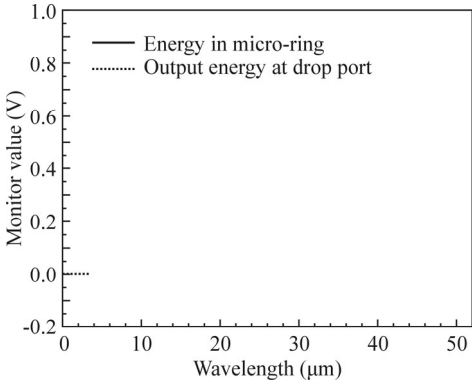

(a) The uncoupling case

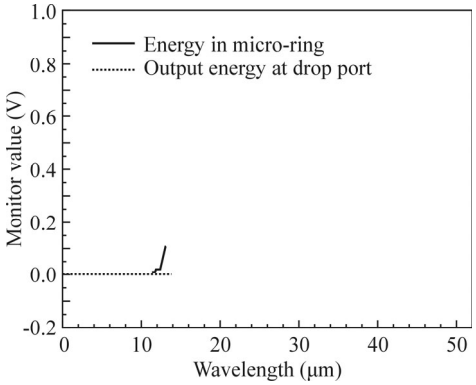

(b) The first energy-coupling case

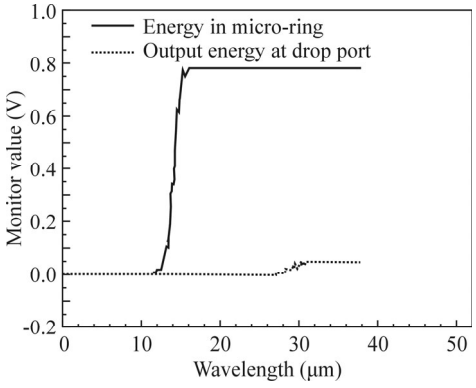

(c) The second energy-coupling case

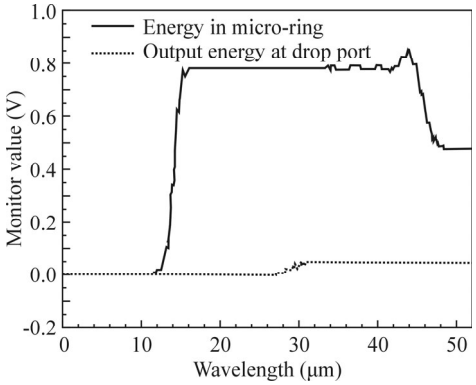

(d) The third energy-coupling case

Fig.6 Transmission spectra corresponding to Fig.4

In summary, we analyze the model of silicon-based micro-ring resonator based on the parallel waveguide structure and its energy transfer. Through these analyses, we get more intuitive transmission lines and energy transfer diagrams. If the input optical signals all satisfy the corresponding resonance condition, there is no output energy at the through port. On the contrary, it can be detected at the through port. Such a circuit can be used as filter, optical switch and light path selector. In addition, it is indicated that optical devices with more functions, higher levels of integration and more flexible structure will be available in the future.

References

[1] H. J. Caulfield and S. Dolev, Nature Photon **4**, 261 (2010).

[2] V. K. Srivastava and V. Priye, Optica Applicata **41**, 157 (2011).

[3] E. A. J. Marcatili, Bell Labs Technical Journal **48**, 2103 (1969).

[4] H. J. Caulfield, R. A. Soref and C. S. Vikram, Photon. Nanostruct. Fundam. Appl. **5**, 14 (2007).

[5] A. I. Zavalin, H. J. Caulfield and C. S. Vikram, Optik **121**, 1300 (2010).

[6] R. Soref, Advanced in Optoelectronics **2011**, 627802 (2007).

[7] GU Guo-qiang, CAI Zhi-ping, XU Hui-ying, WANG Jin-zhang, XU Bin and YAN Yu, Journal of Optoelectronics · Laser **23**, 2267 (2012). (in Chinese)

[8] L. Zhang, J. F. Ding, Y. H. Tian, R. Q. Ji, L. Yang, H. T. Chen, P. Zhou, Y. Y. Lu, W. W. Zhu and R. Min, Optics Express **20**, 11605 (2012).

[9] Shiyun Lin, Yasuhiko Ishikawa and Kazumi Wada, Optics Express **20**, 1378 (2012).

[10] YANG Jian, CHEN Wei-wei, WANG Wan-jun, WANG Ming-hua and YANG Jian-yi, Journal of Optoelectronics · Laser **24**, 16 (2013). (in Chinese)

[11] Liangjun Lu, Linjie Zhou, Xinwan Li and Jianping Chen, Optics Letters **39**, 1633 (2014).

[12] C. Qiu, X. Ye, R. Soref, L. Yang and Q. Xu, Optics Letters **37**, 3942 (2012).

[13] J. Hardy and J. Shamir, Optics Express **15**, 150 (2007).

[14] Yu Jin-zhong, Silicon Photonics, Beijing: Science Press, 227 (2011). (in Chinese)